Cell Cycle–dependent Changes in the Dynamics of MAP 2 and MAP 4 in Cultured Cells

J. B. Olmsted,* D. L. Stemple,‡ W. M. Saxton,‡ B. W. Neighbors,‡ and J. R. McIntosh‡

*Department of Biology, University of Rochester, Rochester, New York; and ‡Department of Molecular, Cellular, and Developmental Biology, University of Colorado, Boulder, Colorado

Abstract. To examine the behavior of microtubule-associated proteins (MAPs) in living cells, MAP 4 and MAP 2 have been derivatized with 6-iodoacetamido-fluorescein, and the distribution of microinjected MAP has been analyzed using a low light level video system and fluorescence redistribution after photobleaching. Within 1 min following microinjection of fluoresceinated MAP 4 or MAP 2, fluorescent microtubule arrays were visible in interphase or mitotic PtK1 cells. After cold treatment of fluorescent MAP 2-containing cells (3 h, 4°C), microtubule fluorescence disappeared, and the only fluorescence above background was located at the centrosomes; microtubule patterns returned upon warming. Loss of microtubule immunofluorescence after nocodozole treatment was similar in MAP-injected and control cells, suggesting that injected fluorescein-labeled MAP 2 did not stabilize microtubules. The dynamics of the MAPs were examined further by FRAP. FRAP analysis of interphase cells demonstrated that MAP 2 redistributed with half-times slightly longer (60 ± 25 s) than those for MAP 4 (44 ± 20 s), but both types of MAPs bound to microtubules in vivo exchanged with soluble MAPs at rates exceeding the rate of tubulin turnover. These data imply that microtubules in interphase cells are assembled with constantly exchanging populations of MAP. Metaphase cells at 37°C or 26°C showed similar mean redistribution half-times for both MAP 2 and MAP 4; these were 3–4 fold faster than the interphase rates (MAP 2, $t_{1/2}$ = 14 ± 6 s; MAP 4, $t_{1/2}$ = 17 ± 5 s). The extent of recovery of spindle fluorescence in MAP-injected cells was to 84–94% at either 26 or 37°C. Although most metaphase tubulin, like the MAPs, turns over rapidly and completely under physiologic conditions, published work shows either reduced rates or extents of turnover at 26°C, suggesting that the fast mitotic MAP exchange is not simply because of fast tubulin turnover. Exchange of MAP 4 bound to telophase midbodies occurred with dynamics comparable to those seen in metaphase spindles ($t_{1/2}$ = ~27 s) whereas midbody tubulin exchange was slow (>300 s). These data demonstrate that the rate of MAP exchange on microtubules is a function of time in the cell cycle.

MICROTUBULE-ASSOCIATED proteins (MAPs)[1] are a group of molecules that were first defined on the basis of their ability to bind to and promote the assembly of tubulin in vitro (for reviews, see references 29 and 48). A number of types of MAPs have now been identified. These include (*a*) the major MAPs from neural tissues (MAP 1, MAP 2, and tau); (*b*) a group of thermostable MAPs of 200–240 kD, originally isolated from cultured cells, and including 210-kD HeLa MAP (6), MAP 4 from mouse neuroblastoma cells and mouse tissues (32, 34), and 205 kD MAP from *Drosophila* (19); and (*c*) a complex group of polypeptides called chartins (26). Immunofluorescent analyses have indicated that most of these MAPs are associated with microtubules in vivo as well as in vitro. However, it is also clear that not all microtubules have an equivalent complement of MAPs. For example, MAP 1 from brain is widely distributed in cultured cells and is found in both neuronal and glial cell types in brain (4). In contrast, MAP 2 is primarily localized to cell bodies and dendrites (1, 8), while tau is in axons (2). MAP 4 has been found in a number of adult mouse tissues, but it is restricted to the microtubules of only a subset of cell types within each tissue (32, 35, 36). MAP 4 also occurs both in oocytes and early mouse embryos, but is absent from mature sperm (32; Olmsted et al., manuscript in preparation).

While the distribution and biochemistry of these MAPs are now becoming clear, little is yet known about how these MAPs act during the assembly and functioning of microtubules in cells. The increased synthesis of MAP 4 (30, 31), MAP 1 (16, 20) and tau (15, 16) during neurite elongation has been interpreted to indicate that these MAPs are significant in the organization of cytoskeletal microtubules during the development of cell asymmetry. Whether these MAPs might potentiate microtubule initiation or organiza-

Portions of this work have appeared in abstract form (1985. *J. Cell Biol.* 101:31a [Abstr.]).

1. *Abbreviations used in this paper*: MAP, microtubule-associated protein.

tion, or stabilize microtubules after polymerization is still not clear. Injection of a monoclonal antibody raised to the 210-kD HeLa MAP into prometaphase cells resulted in the slow dissolution of spindle birefringence and a decrease in the frequency of successful anaphase motions, suggesting a possible function of this MAP in mitotic events (22). However, to develop an understanding of how MAPs interact with tubulin, it will be necessary to study the behavior of these molecules directly in living cells.

During the last several years, the techniques of fluorescence analogue cytochemistry have provided a means for examining the dynamics of molecules in living cells. Several studies (23, 38, 40, 42, 45, 51, 52) have documented that labeled tubulin equilibrates rapidly with existing microtubules in situ. The kinetics of this equilibration have been further analyzed using the technique of fluorescence redistribution after photobleaching (FRAP). Studies on mammalian cells indicate that tubulin molecules exchange surprisingly rapidly with microtubules. This exchange appears to be about ten times faster in mitotic spindles ($t_{1/2}$ ~11–40 s) than in interphase microtubule networks ($t_{1/2}$ ~200 s) (40, 52). While recent work shows that observation and photobleaching of microtubules made with fluorescent tubulin may affect microtubule integrity (50), the swift exchange of tubulin with microtubules in vivo has been shown with diverse methods and is not in doubt (10, 11, 27, 42). Analyses of derivatized MAP 2 injected into cells have also been initiated (41, 49; this report). While MAP 2 does not occur in nonneuronal cell types, injected MAP 2 has been found to co-distribute with microtubule arrays in both interphase and mitotic cells in neuronal and nonneuronal cells. FRAP analyses have suggested that MAP 2 exchanges slowly ($t_{1/2}$ ~5 min) with microtubules in interphase cells (41).

In the current study, we have examined the dynamics of MAP 2 and MAP 4 in both mitotic and interphase cells. While MAP 2 is found largely in cells of neuronal origin, MAP 4 (34, 35) and the 210-kD HeLa MAP (7, 22) are present in diverse cell types and are found in spindles by immunocytochemistry. By comparing the behavior of the two different MAPs with the data on tubulin dynamics obtained previously, we show here that both these molecules exchange with the microtubule surface at rates that vary as a function of time in the cell cycle.

Materials and Methods

Preparation and Derivatization of MAPs

MAP 2. Bovine brain microtubules were obtained by temperature-dependent cycles of assembly-disassembly with (44) or without (5) glycerol. The preparation of derivatized MAP 2 was carried out as described by Scherson et al. (41) except for the modifications listed below.

MAP 4. MAP 4 was prepared from a variety of cells and tissues using one of the following methods:

(*a*) Taxol-driven assembly. Cell extracts (usually mouse neuroblastoma cells, mouse L cells, or HeLa cells) were prepared by homogenization of 1 vol of packed cells with 1 vol of 0.1 M Pipes, 1 mM $MgCl_2$, 1 mM EGTA, 1 mM GTP, pH 6.9 containing 1 mM DTT, 1 μg/ml pepstatin, 1 μg/ml leupeptin, and 1 mM PMSF. After centrifugation at 30,000 *g* for 20 min (18,000 rpm, SS 34 rotor; Sorvall Instruments Div., part of DuPont Co., Newton, CT), the supernatant was removed and centrifuged at 100,000 *g* for 1 h (40,000 rpm, Ty 65 rotor; Beckman Instruments Inc., Palo Alto, CA). Taxol stabilized microtubules were then prepared from these extracts as described by Vallee (47).

(*b*) Incubation of thermostable extracts with taxol-stabilized, MAP-depleted microtubules. Extracts were prepared from mouse tissues (liver, lung, and/or heart) as described above except that tissues were homogenized using a ratio of 1 g tissue/1 ml buffer. The extracts were boiled for 5 min and then chilled to 0°C. After centrifugation at 18,000 rpm for 40 min at 4°C (SS 34 rotor; Sorvall Instruments Div., part of DuPont Co.), the thermostable supernatants were removed and brought to 10 μM in taxol and 1 mM in GTP. The thermostable extract was then mixed with DEAE-purified tubulin (5) from cow brain, or with MAP-stripped microtubules that had been previously prepared by polymerizing cow brain or mouse brain microtubule protein in the presence of 10 μM taxol and 0.5 M NaCl. After incubation for 15 min at 37°C, the mixture was centrifuged at 18,000 rpm for 30 min at room temperature through a 20% sucrose cushion made in 0.1 M Pipes, 1 mM $MgCl_2$, 1 mM EGTA, 1 mM GTP, pH 6.9. The resultant pellet contained "hybrid" microtubules composed of thermostable MAP from mouse tissues, and cow or mouse brain tubulin. These pellets were subsequently used for derivatization with fluorophores.

For derivatization, microtubule preparations were resuspended in 0.3 M 2-(*N*-morpholino) ethane sulfonic acid, 1 mM EGTA, 1 mM $MgCl_2$, pH 6.6, (41) at room temperature. Final protein concentrations used ranged between 5–25 mg/ml, and recovery of labeled material at any of these concentrations was equivalent. MAP 2 preparations were derivatized with 1 μl of 50 mM stock solution of 6-iodoacetamidofluorescein (6-IAF; Molecular Probes, Junction City, OR) in DMSO per milligram protein (approximate ratio of 3 mol IAF/1 mol of microtubule protein) and MAP 4 at a ratio of 10 μl/mg protein (approximate ratio of 30 mol of IAF/1 mol of microtubule protein). After 10 min at room temperature in the dark, the reaction was terminated by the addition of DTT to a final concentration of 2 mM and NaCl to a final concentration of 0.8 M. The material was then passed over a G-25 or G-50 Sephadex column equilibrated in 0.3 M 2-(*N*-morpholino)ethane sulfonic acid, 1 mM $MgCl_2$, 1 mM EGTA, pH 6.6, containing 0.3 M KCl to remove free dye. Pooled column fractions were brought to 2 mM DTT, boiled for 5 min, and then centrifuged at 18 K rpm for 30 min. The resultant supernatant was either used without further concentration (final protein concentration of 50–100 μg/ml) or was concentrated by the addition of saturated ammonium sulfate to 45%. Pellets obtained following ammonium sulfate precipitation were resuspended in 0.3 M 2-(*N*-morpholino)ethane sulfonic acid, 1 mM $MgCl_2$, 1 mM EGTA, pH 6.6, containing 0.3 M KCl and 2 mM DTT to volumes that resulted in final protein concentrations of 0.5–1 mg/ml. Ammonium sulfate precipitated material or column fractions were stored in liquid nitrogen, or for short term (up to 5 d) at 4°C. We found that removal of free dye by chromatography before boiling resulted in a much higher yield of active protein recoverable by ammonium sulfate precipitation than when protein was boiled in the presence of free dye, as described previously (41). The labeling ratios of MAP 4 and MAP 2 prepared by the methods described above were estimated to be ~1–2 mol IAF/1 mol of MAP (see below). Before injection, preparations were recycled onto taxol-stabilized microtubules made with purified tubulin. MAPs were then salt-stripped, boiled, and centrifuged. These further steps removed any derivatized MAPs that were inactive.

In Vitro Assay of Derivatized MAP

To test the activity of derivatized MAP, DEAE-purified tubulin (1–2 mg/ml) was mixed in varying ratios with derivatized MAP (0.1–0.2 mg/ml), and incubated in 0.1 M Pipes, 1 mM $MgCl_2$, 1 mM EGTA, 1 mM GTP, pH 6.9, in the absence of taxol for 15–20 min at 37°C. The incubated material was then sedimented at 37°C (18,000 rpm, SS 34 rotor; Sorvall Instruments Div., part of DuPont Co.). The pellet and supernatant were analyzed on gels for the presence of tubulin and derivatized MAP. The pellet was resuspended in 0.1 Pipes, 1 mM $MgCl_2$, 1 mM EGTA, 1 mM GTP, pH 6.9 + 10 μM taxol, and NaCl was then added to 0.5 M. After centrifugation at 18,000 rpm for 30 min, the resultant supernatant was assessed for MAP content.

Other Biochemical Procedures

Protein samples were analyzed on 5 or 7.5% polyacrylamide gels containing SDS. Gels with fluorescent samples were photographed on a long-wave UV light box (667 film; Polaroid Corp., Cambridge, MA), and were then stained with silver (28). Protein concentrations were determined using the assay from Bio-Rad Laboratories (Cambridge, MA). To estimate coupling ratios, the percentage of MAP in the purest preparations was determined from gel scans, and the amount of fluorescence in the sample was measured in a spectrophotometer by the OD at 490 nm. Photographs of fluorescent gels were scanned to confirm that the majority of fluorescence measured was that associated with MAPs.

Microinjection

PtK1 cells or BSC cells were cultured on glass coverslips, and pressure-injected with fine glass capillary needles as described previously (40). Purified protein for injection was prepared immediately before use by dialysis against PBS, followed by centrifugation in a microfuge for 10 min to remove aggregates. Cells were injected at either room temperature or at 37°C, and were then analyzed after incubation at 37°C for periods ranging between 10 min and 24 h. Derivatized proteins were injected at concentrations between 20 and 500 μg/ml; this range of protein had no detectable effect on the dynamics of MAPs derived from FRAP experiments (see below).

Immunofluorescent Analysis of Nocodozole-treated Cells

PtK1 cells were seeded onto coverslips on which the patterns from a finder grid had been shadowed with gold. All of the cells in selected hexagons of the grid pattern were injected with fluoresceinated MAP 2. Cells were allowed to equilibrate at 37°C between 30 min and 4 h, and individual coverslips were then treated with 18 μM nocodozole for 1, 15, 30, or 60 min. After fixation with −20°C methanol for 5 min and −20°C acetone for 1 min, coverslips were processed for indirect immunofluorescence using a monoclonal antibody to sea urchin tubulin and goat-anti-mouse IgG coupled to rhodamine. Random fields of uninjected cells were photographed and compared with cells that had been injected with fluoresceinated MAP 2. In some experiments, cells injected with derivatized MAPs were fixed as above, photographed, and then processed for immunofluorescence with tubulin antibodies to compare the distribution of the injected MAP relative to microtubules.

FRAP Experiments and Data Analysis

FRAP analyses were carried out to examine the dynamics of MAPs in cells. Cells grown on coverslips were injected, and then mounted for observation in a sealed chamber containing tissue culture medium. Cells were analyzed at either 25–26°C or at 37°C. Temperature was maintained with an air curtain and monitored continuously with a thermistor mounted in the immersion oil on the microscope stage. Regions of injected cells were bleached for 50 or 100 ms with an argon ion laser as described previously (39, 40). Images of injected cells were obtained with a video camera (ISIT; DAGE-MTI, Michigan City, IN), and photographs were taken from the video monitor. Images used for measurements of the cellular fluorescence intensity were collected using a video image processing system built by Hannaway and Associates (Boulder, CO). (For a complete description of the system, see Stemple et al. (46).) The system allowed averages of successive video frames to be calculated and stored as digital video images during the course of a FRAP experiment. Typically, 64 successive video frames, each consisting of arrays of 512 × 480 pixels digitized with 256 gray levels, were averaged into a single image; this average corresponded to a time interval of 2.13 s. For metaphase cells, an image was recorded before bleaching, and a series of images was collected at 1, 7, 18, 25, 40, 80, 160, and 320 s postbleach. For interphase cells, the postbleach pictures were collected at 1, 10, 30, 60, 120, 240, 480, 720, and 960 s.

For analysis of FRAP experiments, the stored images were first transformed on a pixel-by-pixel basis, allowing output voltage to be correlated directly with fluorescence intensity and thereby facilitating measurement of relative intensity from different parts of an image (46). Transformed images were then analyzed by using interactive video graphics programs that allowed the definition of boundaries around the whole cell, the photobleached region, and for metaphase cells, the bleached and unbleached portions of the spindle. Within each region, the average pixel value was calculated and used for comparison with other regions. For interphase cells, the ratio between the bleached region and the whole cells was used. For metaphase cells, the average pixel value of the region outside the spindle was used as the background value of fluorescence in the cell. Ratios were calculated between the bleached half-spindle minus the background and the unbleached half spindle minus the background. The postbleach ratios were normalized to the prebleach ratio, which is assumed to be a measure of the steady state condition for that cell. The normalized ratios from successive time points were then used to describe the redistribution of fluorescence after bleaching. Half time and extent of redistribution were estimated by approximating the recovery with a function of the form: $F = A\,(1 - e^{-kt})$, fit to the data by the method of least squares. The extent of redistribution was estimated by the parameter A, and the half time was estimated from the parameter k using the formula: $t_{1/2} = ln\,(2)/k$.

Results

Preparation and Characterization of Derivatized MAPs

Fluorescence analogue cytochemistry depends upon the preparation of fluorescent proteins that are pure and retain activity. While this had been reported for MAP 2 preparations (41), we found it necessary to develop procedures for the study of MAP 4. In previous work (34), we had demonstrated that MAP 4 was present in a number of tissues from mouse. Heart, lung, and liver contain MAP 4, but not MAP 2, so these tissues were routinely used to prepare thermostable protein fractions for MAP 4 derivatization. When thermostable extracts from these tissues or from microtubule

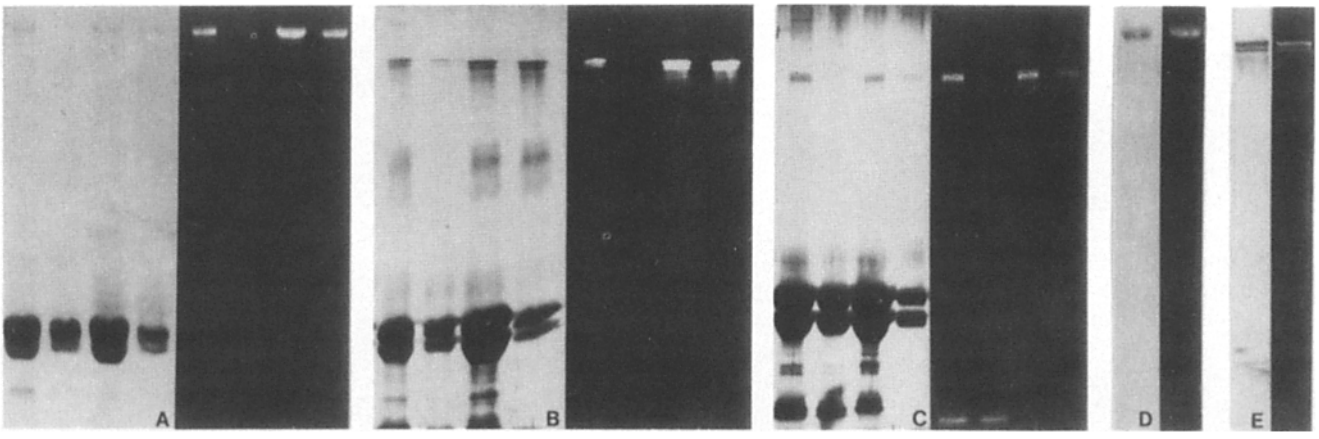

Figure 1. Binding of derivatized MAP to microtubules in vitro. Derivatized MAP fractions were incubated with DEAE-purified tubulin at 37°C in the absence of taxol (first lanes from left in *A*, *B*, and *C*). After centrifugation, the supernatant was removed (second lanes from left) and the pellet of microtubules (third lanes from left) was resuspended with buffer containing 10 μm taxol and 0.5 M NaCl. This materal was centrifuged to pellet microtubules, and the resultant supernatant (fourth lanes from left) contained MAP stripped from the microtubules. The salt-stripped MAP fractions were then reboiled and centrifuged to remove residual tubulin and other contaminants. *D* and *E* show samples typical of those used for injection. The left and right sections in *D* and *E* show a silver stain and fluorescence image, respectively, of the samples. *A* and *D*, beef brain MAP 2; *B* and *E*, mouse lung MAP 4; *C*, HeLa 210-kD MAP.

preparations from cultured cells were mixed with pure tubulin or with salt-stripped, taxol-stabilized microtubules, hybrid microtubules were obtained that were greatly enriched in MAP 4. After derivatization and boiling, MAP 4 was the fluorescently labeled species in the soluble fraction. This material was then used for further assays.

To test whether the derivatized MAPs were biochemically active, we assessed their ability to bind to, and induce the assembly of, tubulin. The properties of derivatized and underivatized MAPs were indistinguishable in all of the in vitro assays used. As shown in Fig. 1, *A–C*, preparations of derivatized MAP 2, MAP 4, or HeLa 210-kD MAP promoted the assembly of DEAE-purified tubulin to form microtubules containing bound MAP. Moreover, taxol could be added to stabilize these microtubules, and then the MAPs could be extracted from the microtubules by treatment with buffer containing 0.5 M NaCl. The ability of the derivatized MAP 4 to promote assembly was seen over a range of molar ratios of MAP/tubulin, and the MAPs were recovered in the pellet (Fig. 1, *A–C*, lane *3*). The conjugation of MAP 4 or HeLa 210-kD MAP with 6-IAF, therefore, appeared to have no detrimental effect on the known in vitro function of this protein, as had previously been shown in similar assays for a preparation containing MAP 2 (41). Routinely, derivatized MAPs that were to be used for injection were bound to taxol-stabilized microtubules made from purified tubulin, sedimented, and then released with salt (similar to sample seen in Fig. 1, *A–C*, lane *4*). Depending upon the volumes used, essentially all or a large fraction of the MAPs in the pellet were released by the salt treatment. In the preparations where this single wash did not appear to give complete recovery (pellet was still slightly yellow), the remainder of the derivatized material was released by rewashing the pellet. For preparations in which the derivatized MAPs bound efficiently to microtubules, there was little evidence for irreversible aggregation of the derivatized material. The resultant supernatant containing the MAPs released by salt treatment was boiled and centrifuged to obtain fully active soluble MAPs with no residual tubulin (Fig. 1, *D* and *E*). These highly purified preparations were used for all injections.

Several types of experiments were carried out to assess the extent to which laser irradiation might affect the behavior of derivatized MAPs. Aliquots of derivatized MAP 2 were bleached to 40–50% of their original fluorescence and compared to unbleached material. Over a range of concentrations (fivefold ratio of MAP/tubulin), both types of preparations were equivalent in promoting the assembly of DEAE-purified tubulin. When microtubules containing derivatized MAPs were bleached in vitro, the MAPs were retained on the microtubules at levels equivalent to the unbleached sample. Bleaching at the high protein concentrations used in these in vitro experiments did result in some aggregation of the protein samples (<15%, as assessed by comparing material trapped at the top of the gel in bleached and unbleached samples). However, the times required for bleaching of preparations in solution (seconds) were much longer than those used for the in vivo analyses (milliseconds). Experiments with tubulin (24) and red blood cell membranes (43) suggest that slow bleaching is more damaging to fluorescent proteins than fast. Therefore, even under conditions which were more likely to be damaging than those in the cell, the data suggest that the bleached MAPs were effective in promoting the assembly of tubulin, and that equivalent amounts of MAPs remained bound to microtubules, regardless of whether they were bleached or not.

Microtubules assembled from fluorescent tubulin in the presence of taxol disintegrate when illuminated by light that excites fluorescence (50). This lability can be visualized by video-enhanced differential interference contrast imaging of microtubule preparations and is dependent on several experimental parameters. The photolability of microtubules formed from phosphocellulose-purified tubulin and fluoresceinated MAP 2 (molar ratio of 20:1) was therefore tested using conditions of illumination that cause taxol-stabilized microtubules made of fluorescent tubulin to dissociate within 25 s (2.5 megawatts/m^2, 488 nm light; see Vigers et al. [50] for details). After 450 s, the microtubules made of fluorescent MAP 2 and unlabeled tubulin had lost all their visible fluorescence, but were still intact as seen with video-enhanced differential interference contrast optics. Therefore, unlike microtubules assembled from fluorescent tubulin, microtubules containing fluorescent MAPs are not photolabile.

Distribution of Microinjected MAP In Vivo

The behavior of fluoresceinated MAPs from different sources was examined by injecting them into a variety of cell types and examining the resulting distribution of fluorescence. We found that the 210 kD HeLa MAP and MAP 4 from mouse tissues, L cells, or neuroblastoma cells showed essentially identical properties. Because these proteins represent species-specific homologues of the same MAP type (29, 34; R. West and J. B. Olmsted, manuscript in preparation), these proteins will be collectively referred to as MAP 4 in the following sections. In preliminary experiments, we found that the patterns and rates of incorporation of both MAP 2 and MAP 4 into a number of cell types (BSC, PtK1, Nb, Chinese hamster ovary, 3T3, HeLa) were similar. Our studies therefore concentrated on PtK1 cells in which both mitotic and interphase microtubule arrays could readily be visualized.

As shown in Fig. 2, the arrangement of fluoresceinated MAP 2 or MAP 4 in interphase cells mimicked the patterns seen after injection of derivatized tubulin (39) or those obtained using indirect immunofluorescence with antibodies. Incorporation into these patterns was rapid. Microtubules at the perimeter of the cell were visible within 1–2 min in cells that had been injected close to the nucleus. As shown in Fig. 2 *B*, arrays of microtubules originating at the centrosomes, as well as those at the perimeter of the cell, were visible. MAPs injected into mitotic cells were concentrated in the spindle to levels above background within seconds of injection.

The rapid appearance of fluorescent arrays in either mitotic or interphase cells is interpreted as a further indication of the activity of the derivatized MAP protein. When preparations that were partially or totally inactive by assay in vitro were injected into living cells, very few microtubule-like patterns were observed. Instead, fluorescent material accumulated in small granules, presumably because of the uptake of the inactive protein into autophagic vacuoles. Cells injected with active preparations retained visible fluorescent patterns for at least 24 h and proceeded normally through the cell cy-

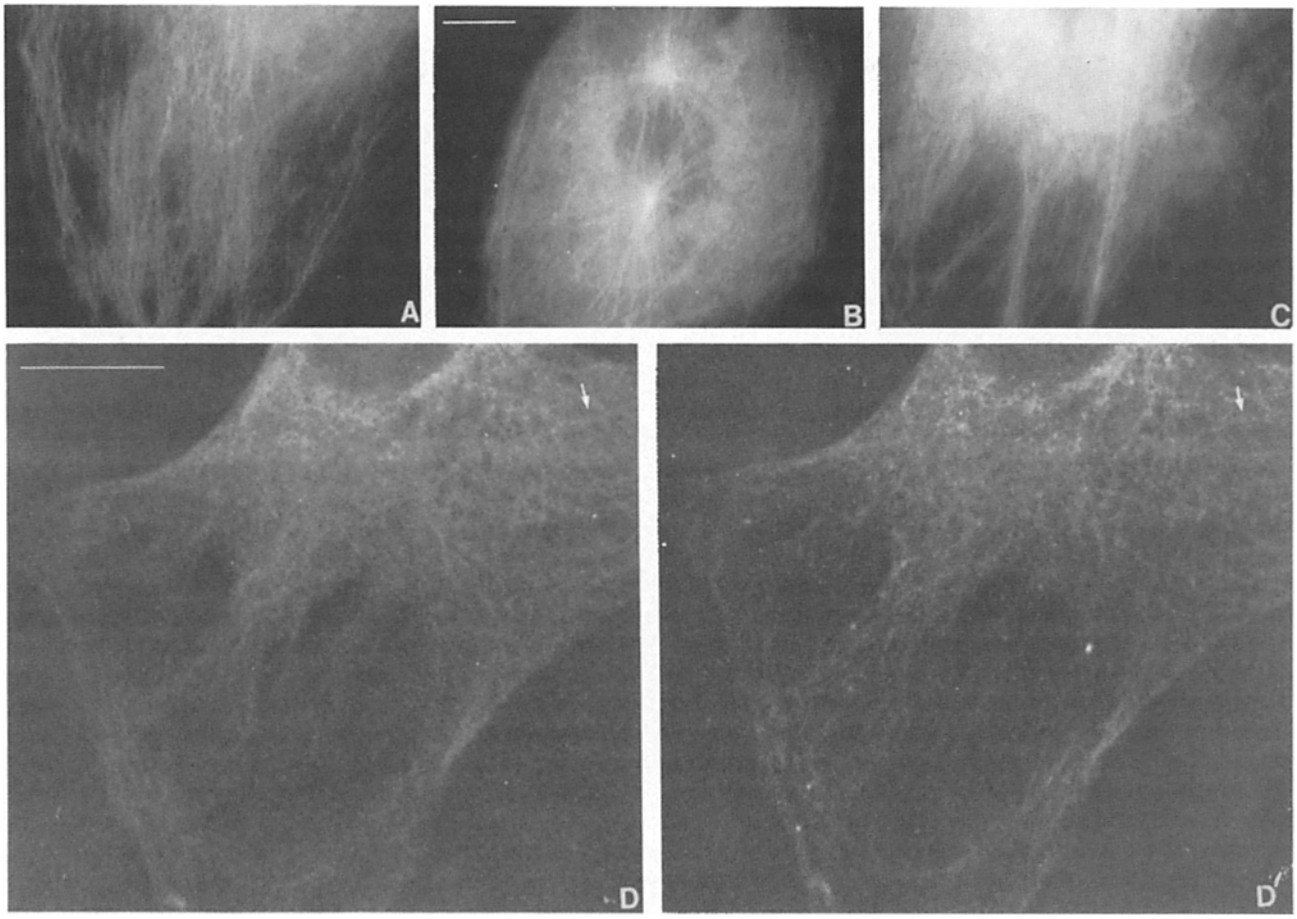

Figure 2. Distribution of microinjected derivatized MAP. PtK1 cells were injected with 6-IAF-derivatized MAP 2 (*A* and *B*) or MAP 4 (*C*) and fluorescence distributions were recorded by taking photographs from a monitor connected to a low light level video camera. A cell injected with derivatized MAP 4 was fixed and photographed directly without image enhancement (*D*), processed for immunofluorescent staining with tubulin antibody and rephotographed to visualize immunolabeled microtubules (*D'*). The photographs have been printed to the same contrast value, although the MAP images are generally much weaker than those seen with tubulin antibody. Note the superposition of the MAP distribution and tubulin staining patterns; arrows mark one of the microtubules visible in both micrographs. Bars, 10 μm.

cle, whether injected during interphase or mitosis. Unlike the recent analyses of cells injected with derivatized tubulin (50), the MAP patterns remained stable over prolonged times of observation; these data are consistent with the in vitro evidence that the microtubules containing derivatized MAPs are not photolabile.

The fluorescence patterns suggested strongly that injected MAPs were associated with microtubules in vivo. This infer-

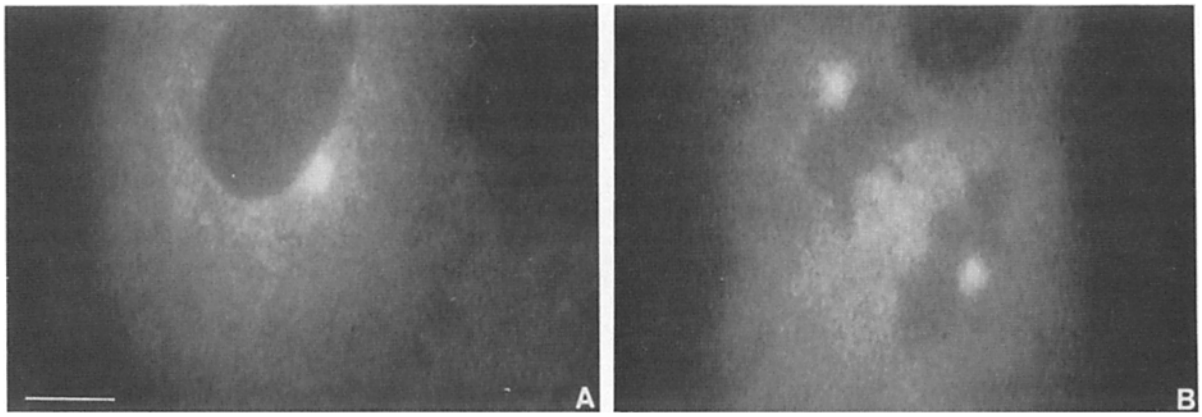

Figure 3. Distribution of MAP 2 after cold treatment. PtK1 cells were injected with MAP 2, left at 37°C for 4 h, and then shifted to 4°C for 3 h. Photographs were taken when cells had been at <15°C for ~1 min. Fluorescence is evenly distributed throughout the cytoplasm except for a concentration of materal in the immediate vicinity of the interphase centrosome (*A*) or metaphase spindle poles (*B*). Bar, 10 μm.

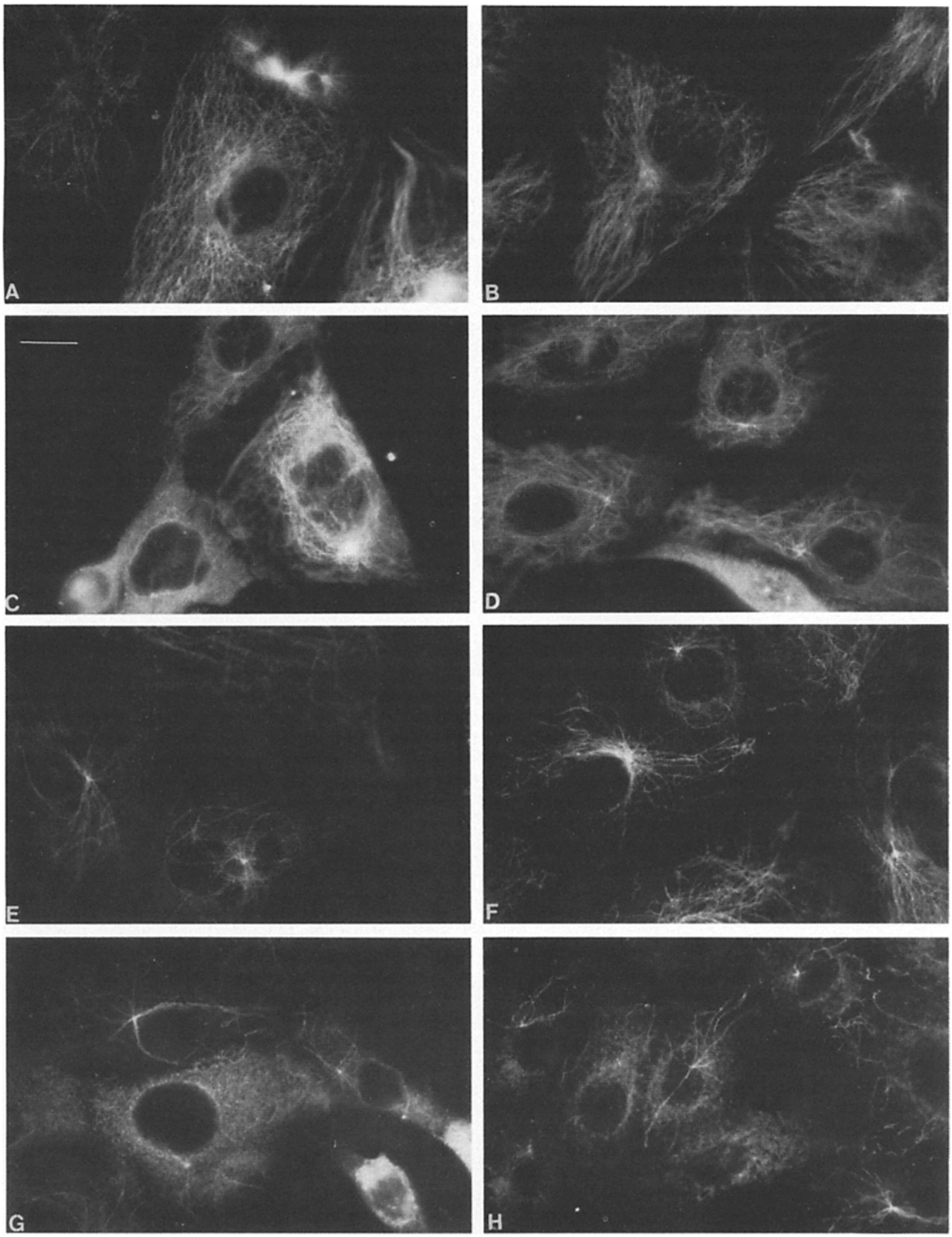

Figure 4. Microtubule distribution in MAP 2–injected and control cells after nocodozole treatment. PtK1 cells were seeded on coverslips. Defined groups of cells were injected with fluoresceinated MAP 2 and then processed for immunofluorescence with tubulin antibody as described in Materials and Methods. Injected (*A*, *C*, *E*, and *G*) and control (*B*, *D*, *F*, and *H*) cells treated with 18 μM nocodozole for 1 min (*A* and *B*), 15 min (*C* and *D*), 30 min (*E* and *F*), and 60 min (*G* and *H*). Note the similarity in the gradual diminution of microtubules in both types of cells with time in nocodozole. Bar, 10 μm.

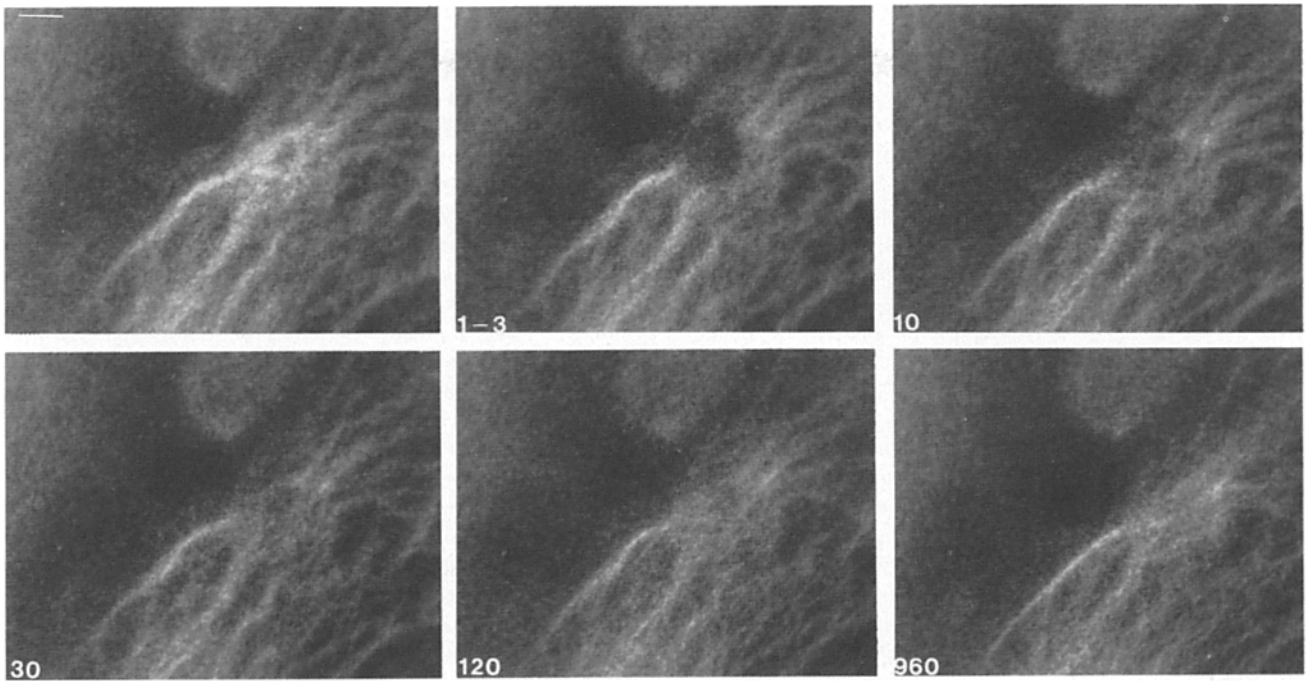

Figure 5. MAP 2 redistribution after photobleaching in an interphase PtK1 cell. Photobleaching was carried out as described in Materials and Methods on an interphase PtK1 cell injected with derivatized MAP 2. The numbers in the lower right of each image denote the time following the bleach at which the image was recorded. The bleaching pulse lasted 50 ms. For the first postbleach picture, a time of 1–3 s is indicated, as the time for recording the image is 2 s. Bar, 5 μm.

ence was tested directly by comparing the patterns seen with injected MAPs and those obtained with tubulin antibodies. Injected cells were fixed and photographed without video enhancement to localize the fluorescence of the injected MAPs. The same cells were then processed for tubulin immunofluorescence. As shown in Fig. 2 *D* and *D'*, the injected MAP 4 pattern is nearly identical with the endogenous microtubules. Similar results were observed for injected derivatized MAP 2 by us (not shown) and others (41). MAP-injected cells were also perturbed with agents known to disrupt microtubules.

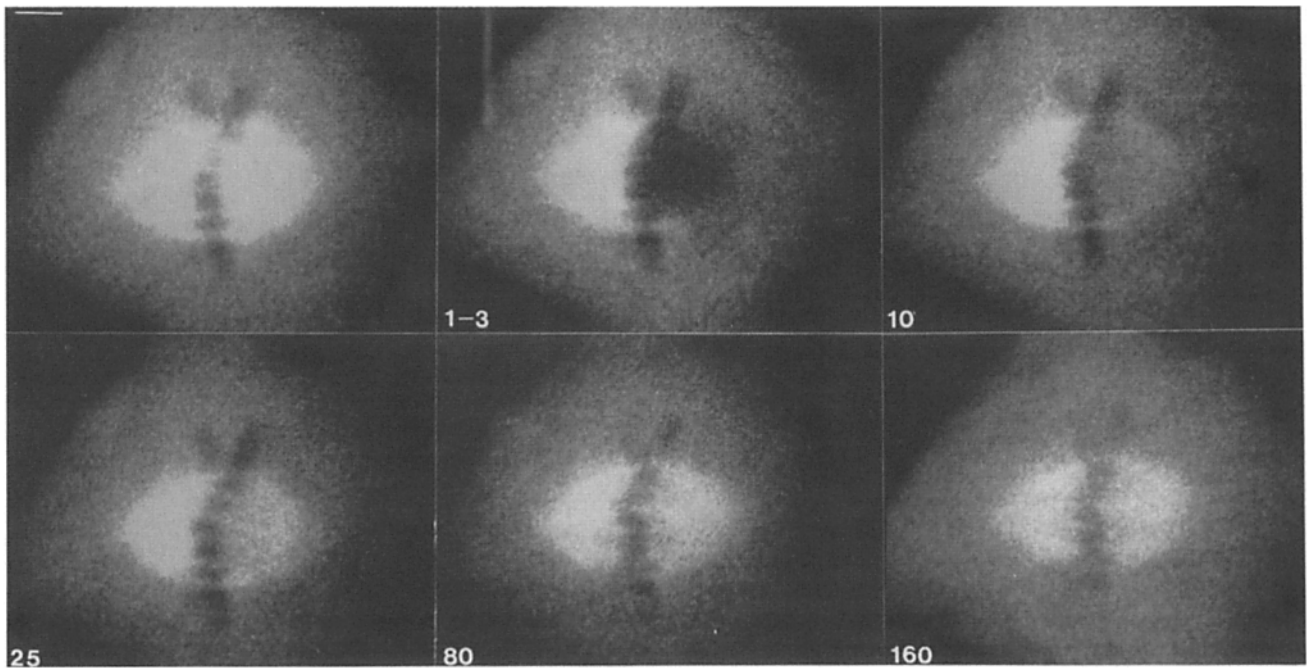

Figure 6. MAP 2 redistribution after photobleaching in a metaphase PtK1 cell. A metaphase PtK1 cell was injected with derivatized MAP 2, and pictures were recorded after photobleaching as described in Fig. 5. Bar, 5 μm.

After incubation with nocodozole, injected cells showed diffuse fluorescence (data not shown). After placing cells injected with MAP 2 into the cold for 3 h, diffuse fluorescence was also observed. After this treatment, however, fluorescence was concentrated in areas corresponding to microtubule organizing centers (centrosomes and spindle poles) in either interphase or mitotic cells (Fig. 3). When cells were injected with fluoresceinated ovalbumin, only diffuse fluorescence was observed, suggesting that the centromeric localization was specific to the MAP. This apparent concentration of MAP 2 may occur because of actual redistribution of MAPs to the microtubule-organizing regions or because such distributions occur normally but are more readily visualized in the absence of the microtubule array. Upon rewarming, microtubule-like arrays originated from these centers (data not shown); similar findings have been reported by Vandenbunder and Borisy (49). While the pattern of microtubule regrowth cannot be directly correlated with the distribution of MAPs in these experiments, our data suggest that MAPs become more evident at microtubule-organizing centers when the normal distribution of microtubules is disrupted.

Effect of Injected MAP on Microtubule Stability in Nocodozole-treated Cells

To determine whether injected MAPs perturbed microtubule distribution or stability, the immunofluorescent pattern of microtubules in control cells was compared with that in cells microinjected with fluoresceinated MAP 2 (Fig. 4). As described in Materials and Methods, all cells within a given hexagon of a finder grid were injected with MAP 2 preparations identical to those used for FRAP analysis, and the presence of the customary pattern of fluorescent MAP was assessed by video imaging. After equilibration at 37°C, the coverslips were treated with nocodozole for various lengths of time. Both injected and control cells on any given coverslip were treated identically with respect to time of equilibration and of nocodozole exposure. The distribution of microtubules in injected cells fixed before nocodozole treatment (not shown) or after 1 min of treatment (Fig. 4, *A* and *B*) was similar, suggesting that the MAP neither augmented assembly, nor caused extensive rearrangement of microtubules. After 15 min of drug treatment, both control (Fig. 4 *D*) and MAP-injected (Fig. 4 *C*) cells showed a diminution in the number of microtubules and an increase in background fluorescence. After 30 min (Fig. 4, *E* and *F*), or 60 min (Fig. 4, *G* and *H*) of treatment, few microtubules were left in either injected or uninjected control cells; the most stable population of microtubules seemed to be a few remnant polymers emanating from the centrosomes. Examination of large numbers of cells indicated that the variation in microtubule patterns among different MAP-injected cells was not different from that seen among control cells, and that on average, the patterns in the two cell types were indistinguishable. These data suggested that injected MAP 2, in contrast to tau (reference 17; see Discussion) did not cause a detectable change in the stability of the microtubules to depolymerization.

Fluorescence Redistribution after Photobleaching

To examine the dynamics of MAP binding in vivo with more precision, FRAP analyses were performed. Several variables were examined in the course of collecting data on a number of cells; none appeared to have any effect on the dynamics measured. The majority of experiments were carried out on PtK1 cells, but results from other cells were similar. Further, MAP dynamics in cells that were observed within 10–15 min of injection were essentially identical to those observed between 3 and 24 h after injection. These data suggest that the parameters being measured were not dependent on a slow equilibration step and that a lengthy recovery after microinjection was unnecessary. The duration of the bleach (50, 100, or 300 ms) had little effect on the dynamics of recovery. Data were also collected using protein preparations that varied in concentration by as much as 10-fold (between 50–500 μg/ml for MAP 2 and 20–200 μg/ml for MAP 4). Variation in the dynamics seen at different concentrations was similar to that seen between different cells at a given concentration, suggesting that the dynamics measured were independent of the concentration injected over the ranges used. For MAP 4, no differences in FRAP rates were observed, regardless of whether the protein injected was isolated from the same species as the recipient cell (HeLa 210-kD MAP), or from a different species (mouse lung or mouse neuroblastoma or L cell MAP 4).

Images typical of those for analysis of interphase and mitotic cells injected with either MAP 2 or MAP 4 are shown in Figs. 5–9. A summary of FRAP data, analyzed as described in Materials and Methods, is presented in Table I. In all cases, the extent of fluorescence recovery after bleaching was to at least 85% of the prebleach value, indicating that photobleaching did not perturb the exchange of derivatized MAP.

The redistribution of MAP 2 or MAP 4 in interphase cells was rapid, and the initial recovery of fluorescence into bleached areas was apparent within 10 s (Figs. 5 and 7). These data are consistent with the qualitative observations on the rapidity with which newly injected MAP assembled into microtubule-like arrays throughout the cell. The fluorescence pattern that was reestablished after bleaching was similar to that seen before bleaching, suggesting that the laser beam did not noticeably disrupt the structure of the microtubules with which the MAPs were interacting. As shown in Table I, there were no significant differences in the redistribution half-times for MAP 2 as compared to those for MAP 4, given the range seen in various cells. However, the dynamics of either of these MAPs were 3–4 fold faster than those previously determined for tubulin using the same experimental system (40) (see Discussion) and the ranges of the values for tubulin and MAPs were essentially nonoverlapping. As measured by *t* test, the probability that the mean half-times for tubulin and either MAP 2 or MAP 4 arise from the same distribution is <0.005. These data suggest strongly that both MAPs exchange with the surface of microtubules in interphase cells.

To assess whether MAP redistribution might occur differently at regions near microtubule organizing centers, areas bleached at the perimeter of the cell were compared to those bleached near the centrosome. Although the abundance of microtubules at the cell center is greater than that at the perimeter, the redistribution half-times for MAP 4 in the two areas were similar. Qualitatively, MAP 2 appeared to have slightly slower redistribution at the perimeter of the cell than at the center, but statistically, the variability among the cell

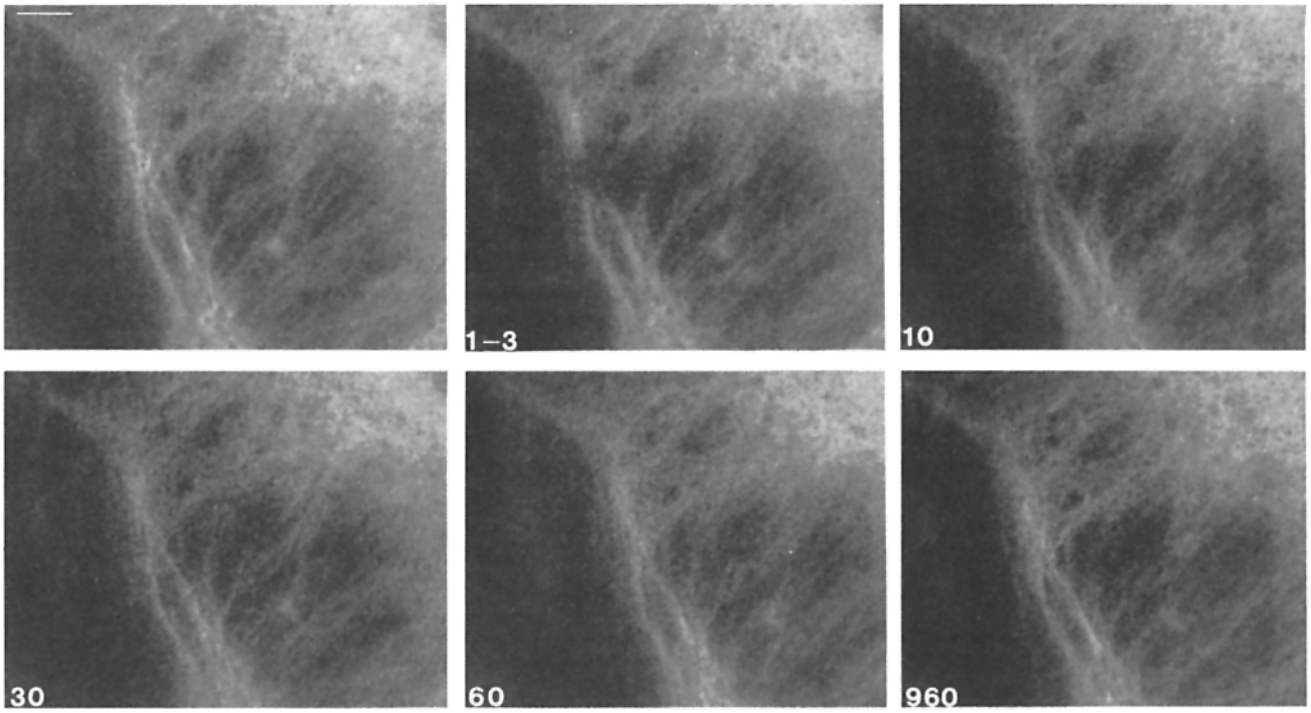

Figure 7. MAP 4 redistribution after photobleaching in an interphase PtK1 cell. An interphase PtK1 cells was injected with derivatized MAP 4, and pictures were recorded after photobleaching as described in Fig. 5. Bar, 5 μm.

samples was sufficiently large that this difference was equivocal. In neither MAP 2 nor MAP 4 injected cells was there any evident polarity to the recovery of fluorescence with respect to the position of fibers in the cell.

FRAP analyses of MAP 2 or MAP 4 in metaphase cells were also undertaken (Figs. 6 and 8). The rates of redistribution for either MAP 2 or MAP 4 in metaphase spindles were rapid, being 3–4 times faster than the dynamics for the MAPs in interphase cells (Table I). These data are consistent with the observation that spindles became fluorescent within seconds after injection of fluoresceinated MAPs. Similar rates of exchange have been found for fluoresceinated tubulin

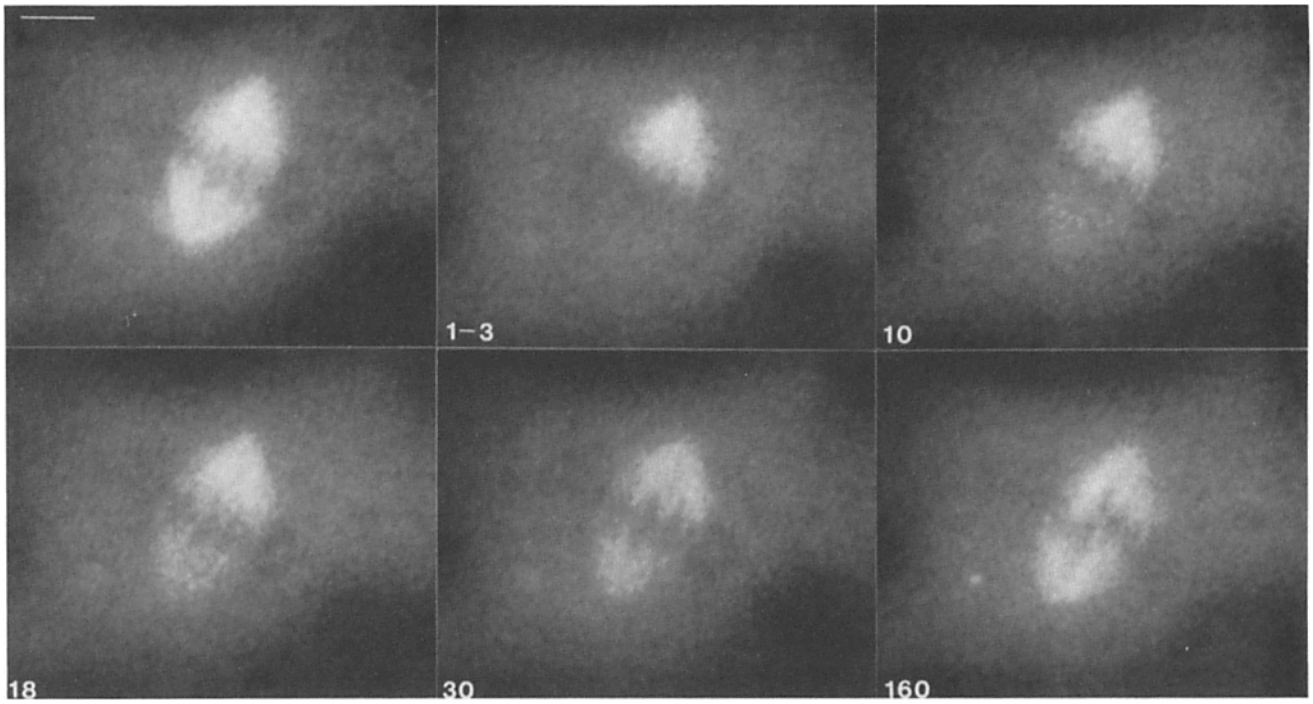

Figure 8. MAP 4 redistribution after photobleaching in a metaphase PtK1 cell. A metaphase PtK1 cell was injected with derivatized MAP 4, and pictures were recorded after photobleaching as described in Fig. 5. Bar, 10 μm.

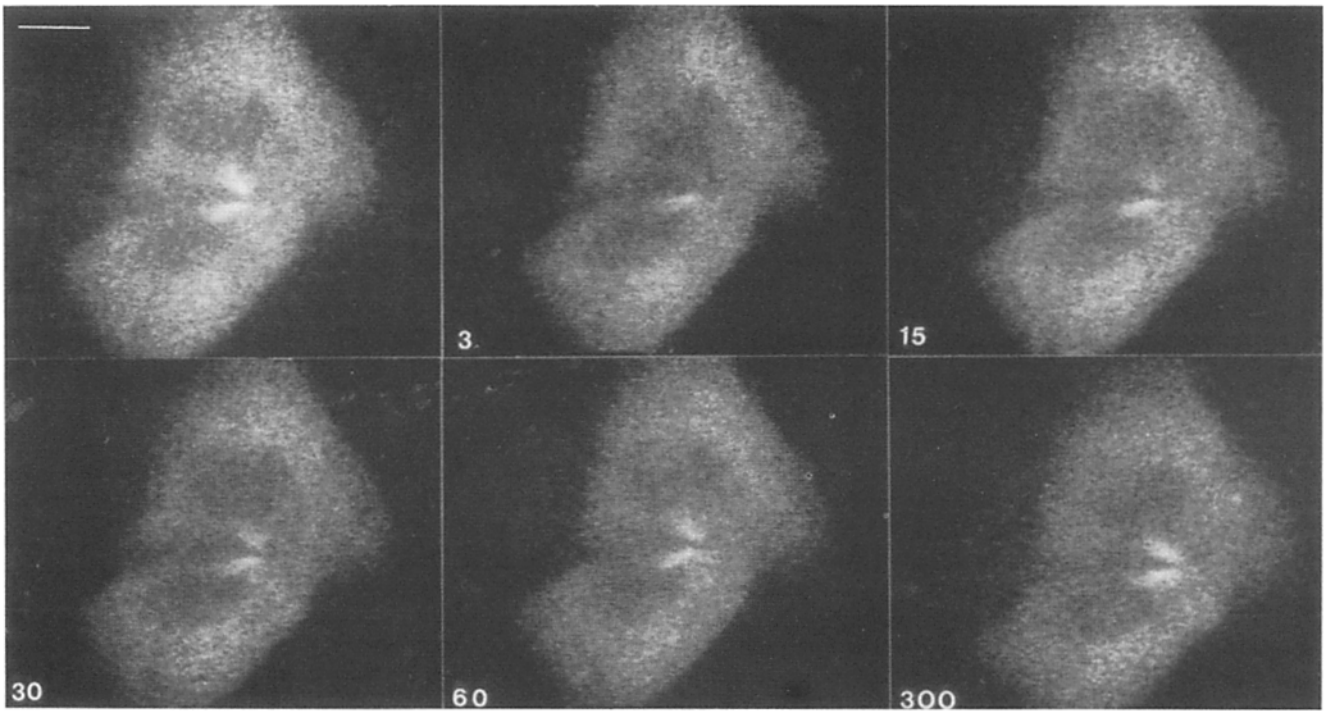

Figure 9. MAP 4 redistribution after photobleaching in the midbody of a dividing PtK1 cell. A PtK1 cell was injected in metaphase with derivatized MAP 4, and then photobleached during cytokinesis. Pictures were recorded as described in Fig. 5. Bar, 10 μm.

in both sea urchin (38) and mammalian (40) spindles. Thus, in contrast to results on interphase cells, both MAPs and tubulin in spindles at 37°C appear to exchange rapidly between structure-bound and free forms.

Experiments were carried out to examine whether cells in transition from mitosis to interphase showed a change in MAP dynamics. Injected MAP 4 associated rapidly with microtubules in midbodies (Fig. 9). FRAP analyses demonstrated that MAP 4 exchanged almost as rapidly in this structure as in metaphase spindles ($n = 4$, $t_{1/2} = 28 \pm 6$ s, range 24–37). This was a surprising result, since tubulin dynamics in the midbody are significantly slower than those observed for either metaphase spindles or interphase microtubule arrays, showing essentially no recovery of general fluorescence 5 min after bleaching (39). These data further support the idea that MAP and tubulin dynamics are separable and that both depend on cell cycle stage.

Table I. Half Times of Recovery of Map 2 and Map 4 after Photobleaching

	n	$t_{1/2}$(s) (mean ± SD)	Range
MAP 2			
Interphase	20	60 ± 25	37–118
Centrosome	14	52 ± 15	37–87
Perimeter	6	81 ± 33	41–118
Metaphase, 37°C	15	14 ± 6	4–24
Metaphase, 26°C	10	13 ± 3	8–18
MAP 4			
Interphase	33	44 ± 20	18–25
Centrosome	26	42 ± 15	18–73
Perimeter	7	48 ± 34	31–125
Metaphase, 37°C	21	17 ± 5	8–24
Metaphase, 26°C	22	14 ± 4	8–24
Tubulin*			
Interphase	4 (PtK1)	270 ± 73	–
	17 (BSC)	200 ± 82	92–320
Metaphase, 37°C	10 (PtK1)	11 ± 6	3–22
	4 (BSC)	13 ± 7	–

* Data from Saxton et al. (40) using 5-(4,6 dichlorotriazinyl)aminofluorescein tubulin.

Experiments were carried out to examine whether there was a change in the kinetics of MAPs in cells in which mitosis was slowed by lowering the temperature to 25–26°C (37). Surprisingly, the rates obtained for MAPs at 26°C were essentially identical to those obtained at 37°C (Table I); further, the extent of fluorescence recovery was at least 90% for cells at either temperature. This is in contrast to data obtained for tubulin, which were more complex (46). The rates of redistribution of tubulin were in the same range for cells at 26°C or 37°C, but the extent of redistribution in cells at 26°C was significantly less than that at 37°C (~60% as opposed to >90%). These data suggest that a population of microtubules has ceased to turnover quickly in the mitotic cells at 26°C. Mitotic MAPs on the other hand, exchange rapidly at either temperature, regardless of the dynamics of the microtubules with which they are associated.

Discussion

The value of fluorescence analogue cytochemistry for examining behavior of molecules in cells is dependent on the extent to which the fluorophore-conjugated protein retains properties typical of the underivatized molecules. As initially demonstrated by Scherson et al. (41), MAP 2 can be

conjugated with 6-iodoacetamidofluorescein and retain both in vitro microtubule binding and assembly promoting activities. In this report, we demonstrate that 6-IAF is also a suitable fluorophore for preparing active, derivatized MAP 4. Our assays have also demonstrated that the bleaching of fluoresceinated MAPs has no effect on their observable activity in vitro. Further, prolonged bleaching of derivatized MAP complexed with microtubules does not affect the stability of individual microtubules, as assessed by video-enhanced microscopy. This contrasts with the recent finding that microtubules prepared with fluorescent tubulin disintegrate upon photobleaching in vitro (50). Since the bleaching of derivatized MAPs does not detectably perturb microtubule integrity under similar experimental conditions, the dynamics observed with this material are likely to be a close approximation of the real rates of exchange of bound and soluble MAP in vivo.

Examination of cells microinjected with MAP 2 or 4 shows that these molecules equilibrate rapidly into arrays resembling those seen both with injected 5-(4,6 dichlorotriazinyl)aminofluorescein tubulin and by immunofluorescence with tubulin antibodies. We as well as others (18, 41, 49) have shown by immunofluorescence that microinjected MAPs of various types associate with microtubules in situ, regardless of whether or not the MAPs injected occur naturally within the types of cells injected. For example, PtK1 cells (22) and BSC cells (7) contain protein antigenically related to the 210-kD HeLa MAP, but there is no evidence for the presence of MAP 2 in either of these cell types. Nonetheless, both these MAPs will bind to microtubules in vivo, and they show similar rates of FRAP. Thus, it may be that certain functionally important regions of these molecules, such as the microtubule binding domain, are conserved in vivo. Such a conserved domain might be significant in explaining why the dynamics of these different MAPs are all similar, irrespective of their origin.

An alternative explanation for the distributions seen is that the injected MAPs bind to endogenous MAPs already bound to the surface of microtubules. The rapid half-times of exchange could then be because of low affinity interactions between MAPs, rather than bonds with the microtubule surface. Although there is currently no way to assess the MAP composition or saturation binding of microtubules in vivo, at least two arguments suggest that this hypothesis could not explain all of the data. First, we (J. Sterner and J. B. Olmsted, unpublished results) have recently microinjected the projection domain of derivatized MAP 2. This fragment, which lacks the microtubule binding domain, does not localize to microtubules, suggesting that interactions with MAPs on the surface of microtubules does not account for the patterns seen with intact MAP 2. Further, one can make a rough calculation, at least for MAP 4, as to whether there are sufficient microtubule binding sites for the injected MAPs even in the presence of the endogenous pool. Most cells contain ~3–4 pg of tubulin at 2 mg/ml; ~50% of this is polymer (21). Assuming that 10% of the cell volume was introduced into the cell during a normal injection, a maximum internal concentration of added MAP in the range of 20–50 μg/ml would be achieved. We have estimated the cellular concentration of MAP 4 in differentiated neuroblastoma cells, which contain high amounts of this MAP to be ~10 μg/ml, and in vitro assays suggest saturation for this protein is ~1 molecule/100 tubulin dimers (J. B. Olmsted, unpublished results). These data suggest that adequate microtubule binding sites exist for the exchange of the MAPs, whether heterologous or homologous, on the surface of the microtubules.

Given the assembly-promoting properties of MAPs in vitro, one might predict that the monomer-polymer distribution of the tubulin pool in vivo would be perturbed by an increase in the cellular concentrations of MAPs, and obvious changes in microtubule-based events would result. However, Vandenbunder and Borisy (49) noted that injected MAP 2 does not alter the duration of any mitotic stage, nor the transition from interphase to prophase and the formation of daughter cells. We too saw no change in cellular microtubule arrangement or microtubule-dependent function following injection of either MAP 2 or MAP 4. Further, as shown by our experiments as well as those of others (41, 49), MAP-decorated microtubules are still labile to disruptive treatments, indicating that an increased cellular concentration of these MAPs has no perceptible effect on microtubule stability. There are at least two likely interpretations of these results. One is that the cell can tolerate minor changes in tubulin monomer-polymer pool without parameters measurable in these experiments being affected. Alternatively, the cell may adjust the affinity of MAP 2 or 4 for microtubules to achieve an amount of polymer that is appropriate for normal cell behavior.

In contrast to these data on high molecular weight MAPs, Drubin and Kirschner (17) have reported that tau protein injected into cells augments both the extent of assembly and stability of microtubules. MAP 2 and tau have recently been shown to share a microtubule-binding motif (25), so one might expect these two proteins to have similar interactions with microtubules. One possible explanation for the differences in the stabilization properties of these two molecules is that the experiments with tau were carried out with underivatized molecules, whereas ours were carried out with derivatized MAP 2. Although all of the in vitro criteria suggest that the derivatized MAP 2 is similar to the underivatized molecule, subtle alterations in structure that affect the cellular behavior cannot be ruled out. However, there are several lines of experimental evidence to corroborate the idea that the interaction of tau and MAP 2 with the microtubule surface may be significantly different. For example, kinetic analyses (9, 14) suggest that MAP 2 is important in the formation of oligomers early in assembly, whereas tau appears to bind preferentially to formed polymers (12). Connolly and Kalnins (13) noted that proteins reacting with tau antibodies were not as readily removed from permeabilized cells as those reacting with antibodies to the high molecular weight MAPS. Both Scherson et al. (41) and we (unpublished results) have noted that it is more difficult to visualize injected MAP 2 once cells are permeabilized. In contrast, the injected tau molecules appear to be tightly associated with microtubule arrays after fixation and permeabilization (17). The two classes of MAPs also show different stabilities in situ. MAP 2 or MAP 4 can be seen bound to microtubules for at least 24 h after injection (these data); in contrast, Drubin and Kirschner (17) noted that tau could not be visualized 3 h after injection, presumably because of degradation. It will be useful to extend these immunofluorescence analyses with FRAP data to determine whether these two classes of MAPs show further differences in vivo.

We have shown that the turnover rate of MAPs 2 and 4 during interphase exceeds that of tubulin, as measured by FRAP, by about threefold, suggesting that MAPs exchange with the microtubule surface in vivo. However, since it has now been shown that the estimates for tubulin exchange established by FRAP analyses may be complicated by perturbations of the derivatized molecules by photobleaching (50), examination of rates of turnover for tubulin established using other procedures are important to consider. In cells treated with nocodozole, half-times for disassembly of tubulin have been estimated as 95 s for PtK1 cells, and 160 s for BSC cells (L. Cassimeris, P. Wadsworth, M. Tioran, E. D. Salmon, unpublished results). These may actually be underestimates of the tubulin disassembly rates. Recent in vitro work indicates that in low concentrations of polymerizable tubulin, the rapid shortening phase of microtubule dynamic instability is rarely rescued, while rescue at steady state is common (53). Studies in which microtubule dynamics have been followed after injection of biotinylated tubulin into interphase BSC cells have indicated that microtubules turn over with half-times of >300 s (42). Thus, regardless of the method that has been used for analysis, the turnover half-times for tubulin appear to be at least 2–4 times longer than those that we have measured for MAPs 2 and 4. Interphase MAPs must therefore be exchanging with microtubules. Even with these slow rates for tubulin, however, one might be concerned that the injected MAPs perturb the turnover of tubulin, so that the MAP turnover in MAP-injected cells might be showing only microtubule behavior. Our data suggest, however, that the injected MAPs do not change the stability of the cell's microtubules. Even if some subtle form of tubulin stabilization results from the injection, the dynamics for tubulin should be *slowed* by the presence of exogenous MAPs. There may be, therefore, an even greater difference between MAP and tubulin dynamics in interphase than is suggested by a comparison of our studies with published work on tubulin in the same cells (40).

The dynamics for MAP 2 that we observed in interphase cells were approximately fivefold faster than those reported by Scherson et al. (41). Some of this discrepancy may arise from differences in the extent of derivatization that affect the properties of the protein, the purity of the preparations injected, or the way in which the data were analyzed. However, it is evident that the recovery observed by Scherson et al. (41) in neurites of neuroblastoma cells (e.g., Fig. 7 in reference 41) was enough slower than that observed for microtubules in the perimeter of PtK1 cells (Fig. 5) that the data are incompatible. An interesting possibility for these differences is that neurite microtubules may be more stable than the polymers in dividing cells, and that this stability may be reflected in MAP dynamics. For example, microtubules in the neurites of highly differentiated PC12 cells are more stable to depolymerization than those in less differentiated cells (3) and biochemical assays have demonstrated that this parallels an increase in the synthesis of endogenous MAPs during differentiation (15, 16, 17). More detailed analysis of tubulin and MAP dynamics in cycling interphase cells versus those that are terminally differentiated should determine whether differentiation affects cytoskeletal protein dynamics.

There is a significant increase in the turnover rates of MAPs and tubulin upon entry of cells into mitosis. In metaphase cells analyzed at 37°C, both MAP 2 and MAP 4 showed dynamics with half times 3–4-fold faster than those for interphase cells. Such rates are similar to those obtained for the exchange of DTAF-tubulin in spindles (40, 52). We found, however, that the dynamics of tubulin and MAP molecules could be separated into readily distinguishable behaviors under conditions where the microtubules to which the MAPs are bound are stabilized by natural (the midbody) or experimental (metaphase cells at 26°C) conditions. Fast exchange of MAP 4 with static microtubules is seen in the midbody, while the tubulin in this structure exchanges extremely slowly (39). Further, at 25–26°C, the progression of PtK1 cells through mitosis is slowed by a factor of 8–12 (37). Both we (this report and reference 46) and Wadsworth and Salmon (52) have found that the extent of tubulin exchange also decreases with temperature. From an analysis of the rate curves, Stemple et al. (46) have suggested that there is a population of microtubules in the spindle that are as dynamic as those in spindles at 37°C, but that there is another population that is static over the time course of the experiments. Our data demonstrate that both MAP 2 and MAP 4 could exchange equally rapidly with both of these populations. These results suggest that there is a spectrum of tubulin dynamics from prophase to cytokinesis, and that the cell can alter the bonds between MAPs and microtubules to modulate the rates of MAP binding and release.

The FRAP analyses demonstrate that the dynamics of MAPs and tubulin are both modulated as a function of the cell cycle. This modulation acts on all the types of MAPs we injected, suggesting that the cell is capable of modifying the interaction of microtubule-binding proteins with microtubules independently of their natural occurrence in the cells. This could mean either that the cell modifies the tubulin, not the MAPs, or that the MAPs studied share properties that make them substrates for the modification system.

The question still remains as to whether MAP and tubulin dynamics are causally linked in cells. The bulk of in vitro experiments have led to the concept that MAPs promote tubulin assembly, and stabilize formed microtubules. Our data indicate that MAPs do not parallel tubulin dynamics at all stages of the cell cycle, and that the rates of association and dissociation of MAPs with microtubules may not be causally linked to the behavior of the tubulin subunits. How these more subtle interactions may be regulated should be directly testable by examining the behavior of injected fragments of MAPs, or modified MAPs, on the dynamics of both MAPs and tubulin in vivo.

J. B. Olmsted is very grateful for the generous hospitality and enthusiastic collaboration of the whole McIntosh laboratory during the sabbatical periods in which these experiments were performed. We thank G. Vigers for his help with the experiments testing the photolability of microtubules that contain fluorescent MAP 2. The taxol used in these studies was provided by the Division of Natural Products, National Cancer Institute, Rockville, MD.

These studies were supported by grants GM 22214 (to J. B. Olmsted) and GM 33787 (J. R. McIntosh) from the National Institutes of Health.

References

1. Bernhardt, R., and A. Matus. 1984. Light and electron microscopic studies of the distribution of microtubule-associated protein 2 in rat brain: a difference between dendritic and axonal cytoskeletons. *J. Comp. Neurol.* 226:203–231.
2. Binder, L. I., A. Frankfurter, and L. I. Rebhun. 1985. The distribution of tau polypeptides in the mammalian central nervous system. *J. Cell Biol.*

101:1371–1378.
3. Black, M., and L. A. Greene. 1982. Changes in the colchicine susceptibility of microtubules associated with neurite outgrowth: studies with nerve growth factor responsive PC12 pheochromocytoma cells. *J. Cell Biol.* 95:379–386.
4. Bloom, G. S., T. A. Schoenfeld, and R. B. Vallee. 1984. Widespread distribution of the major polypeptide components of MAP 1 (microtubule-associated protein 1) in the nervous system. *J. Cell Biol.* 98:320–330.
5. Borisy, G. G., J. M. Marcum, J. B. Olmsted, D. B. Murphy, and K. A. Johnson. 1975. Purification of tubulin and of associated high molecular weight proteins from porcine brain and characterization of microtubule assembly in vitro. *Ann. NY Acad. Sci.* 253:107–132.
6. Bulinski, J. C., and G. G. Borisy. 1979. Self-assembly of microtubules in extracts of cultured HeLa cells and the identification of HeLa microtubule-associated proteins. *Proc. Natl. Acad. Sci. USA.* 76:293–297.
7. Bulinski, J. C., and G. G. Borisy. 1980. Widespread distribution of a 210,000 mol wt microtubule-associated protein in cells and tissues of primates. *J. Cell Biol.* 87:802–808.
8. Caceres, A., M. R. Payne, L. I. Binder, and O. Steward. 1983. Immunocytochemical localization of actin and microtubule associated protein MAP 2 in dendritic spines. *Proc. Natl. Acad. Sci. USA.* 80:1738–1742.
9. Carlier, M. F., C. Simon, and D. Pantaloni. 1984. Polymorphism of tubulin oligomers in the presence of microtubule-associated proteins. Implications in microtubule assembly. *Biochemistry.* 23:1582–1590.
10. Cassimeris, L., N. K. Pryer, and E. D. Salmon. 1988. Real-time observations of microtubule instability in living cells. *J. Cell Biol.* 107:2223–2231.
11. Cassimeris, L., P. Wadsworth, and E. Salmon. 1986. Dynamics of microtubule depolymerization in monocytes. *J. Cell Biol.* 102:2023–2032.
12. Cleveland, D. W., S. Y. Hwo, and M. Kirschner. 1977. Purification of tau, a microtubule-associated protein that induces assembly of microtubules from purified tubulin. *J. Mol. Biol.* 116:207–225.
13. Connolly, J., and V. Kalnins. 1980. Tau and HMW microtubule-associated proteins have different microtubule binding sites in vivo. *Eur. J. Cell Biol.* 21:296–300.
14. Diez, J., J. de La Torre, and J. Avila. 1985. Differential association of the different brain microtubule proteins in different in vitro assembly conditions. *Biochim Biophys. Acta.* 838:32–38.
15. Drubin, D., M. Kirschner, and S. Feinstein. 1984. Microtubule-associated tau protein induction by nerve growth factor during neurite outgrowth in PC12 cells. *In* Molecular Biology of the Cytoskeleton. Cold Spring Harbor Laboratory, Cold Spring Harbor, NY. 343–356.
16. Drubin, D., S. Feinstein, E. Shooter, and M. Kirschner. 1985. Nerve growth factor-induced outgrowth of PC12 cells involves the coordinate induction of microtubule assembly and assembly-promoting factors. *J. Cell Biol.* 101:1799–1807.
17. Drubin, D. G., and M. W. Kirschner. 1986. Tau protein function in living cells. *J. Cell Biol.* 103:2739–2746.
18. Drubin, D., S. Kobayashi, and M. Kirschner. 1986. Association of tau protein with microtubules in living cells. *Ann. NY. Acad. Sci.* 466:257–268.
19. Goldstein, L. S. B., R. A. Lymon, and J. R. McIntosh. 1986. A microtubule-associated protein from Drosophila melanogaster: identification, characterization, and isolation of coding sequences. *J. Cell Biol.* 102: 2076–2087.
20. Greene, L. A., R. K. Liem, and M. L. Shelanski. 1983. Regulation of a high molecular weight microtubule-associated protein in PC 12 cells by nerve growth factor. *J. Cell Biol.* 96:76–83.
21. Hiller, G., and K. Weber. 1978. Radioimmunoassay for tubulin: a quantitative comparison of the tubulin content of different established tissue culture lines and tissues. *Cell.* 14:795–804.
22. Izant, J. G., J. A. Weatherbee, and J. R. McIntosh. 1983. A microtubule-associated protein antigen unique to mitotic spindle microtubules in PtK1 cells. *J. Cell Biol.* 96:424–434.
23. Keith, C. H., J. R. Feramisco, and M. Shelanski. 1981. Direct visualization of fluorescein-labeled microtubules in vitro and in microinjected fibroblasts. *J. Cell Biol.* 88:234–240.
24. Leslie, R. J., W. M. Saxton, T. J. Mitchison, B. Neighbors, E. D. Salmon, and J. R. McIntosh. 1984. Assembly properties of fluorescein-labeled tubulin in vitro before and after fluorescence bleaching. *J. Cell Biol.* 99:2146–2156.
25. Lewis, S. A., D. Wang, and N. J. Cowan. 1988. Microtubule-associated protein MAP 2 shares a microtubule binding motif with tau protein. *Science (Wash. DC).* 242:936–939.
26. Magendantz, M., and F. Solomon. 1985. Analyzing the components of microtubules: antibodies against chartins, associated proteins from cultured cells. *Proc. Natl. Acad. Sci. USA.* 82:6581–6585.
27. Mitchison, T., L. Evans, E. Schulze, and M. Kirschner. 1986. Sites of microtubule assembly and disassembly in the mitotic spindle. *Cell.* 45:515–527.
28. Morrissey, J. H. 1981. Silver stain for proteins in polyacrylamide gels: a modified procedure with enhanced uniform sensitivity. *Anal. Biochem.* 117:307–310.
29. Olmsted, J. B. 1986. Microtubule-associated proteins. *Annu. Rev. Cell Biol.* 2:419–455.
30. Olmsted, J. B., and H. D. Lyon. 1981. A microtubule-associated protein specific to differentiated neuroblastoma cells. *J. Biol. Chem.* 256:3507–3511.
31. Olmsted, J. B., J. V. Cox, C. F. Asnes, L. M. Parysek, and H. D. Lyon. 1984. Cellular regulation of microtubule organization. *J. Cell Biol.* 99(Suppl.):28s–32s.
32. Olmsted, J. B., C. F. Asnes, L. M. Parysek, H. D. Lyon, and G. M. Kidder. 1986. Distribution of MAP 4 in cells and in adult and developing mouse tissues. *Ann. NY. Acad. Sci.* 466:292–305.
33. Deleted in proof.
34. Parysek, L. M., C. F. Asnes, and J. B. Olmsted. 1984. MAP 4: occurrence in mouse tissues. *J. Cell Biol.* 99:1309–1315.
35. Parysek, L. M., J. J. Wolosewick, and J. B. Olmsted. 1984. MAP 4: a microtubule-associated protein specific for a subset of tissue microtubules. *J. Cell. Biol.* 99:2287–2296.
36. Parysek, L. M., M. DelCerro, and J. B. Olmsted. 1985. Microtubule-associated protein 4 antibody: a new marker for astroglia and oligodendroglia. *Neuroscience.* 15:869–876.
37. Rieder, C. 1981. Effects of hypothermia (20-25°C) on mitosis in PtK1 cells. *Cell Biol. Int. Rep.* 5:563–573.
38. Salmon, E. D., R. Leslie, W. M. Saxton, M. L. Karow, and J. R. McIntosh. 1984. Spindle microtubule dynamics in sea urchin embryos: analysis using a fluorescein-labeled tubulin and measurements of fluorescence redistribution after laser photobleaching. *J. Cell Biol.* 99:2165–2174.
39. Saxton, W. M., and J. R. McIntosh. 1987. Interzone microtubule behavior in late anaphase and telophase spindles. *J. Cell Biol.* 105:875–886.
40. Saxton, W. M., D. L. Stemple, R. J. Leslie, E. D. Salmon, M. Zavortink, and J. R. McIntosh. 1984. Tubulin dynamics in cultured mammalian cells. *J. Cell Biol.* 99:2175–2186.
41. Scherson, T., T. E. Kreis, J. Schlessinger, U. Littauer, G. G. Borisy, and B. Geiger. 1984. Dynamic interactions of fluorescently labeled microtubule-associated proteins in living cells. *J. Cell Biol.* 99:425–434.
42. Schulze, E., and M. Kirschner. 1986. Microtubule dynamics in interphase cells. *J. Cell Biol.* 102:1020–1031.
43. Sheetz, M. P., and D. E. Koppel. 1979. Membrane damage caused by irradiation of fluorescent concanavalin A. *Proc. Natl. Acad. Sci. USA.* 76:3314–3317.
44. Shelanski, M. L., F. Gaskin, and C. R. Cantor. 1973. Assembly of microtubules in the absence of added nucleotide. *Proc. Natl. Acad. Sci. USA.* 70:765–768.
45. Soltys, B., and G. G. Borisy. 1985. Polymerization of tubulin in vivo: direct evidence for assembly onto microtubule ends and from centrosomes. *J. Cell Biol.* 100:1682–1689.
46. Stemple, D. L., S. Sweet, M. Welsh, and J. R. McIntosh. 1988. Dynamics of a fluorescent calmodulin analog in the mammalian mitotic spindle at metaphase. *Cell Mot. Cytoskeleton.* 9:231–242.
47. Vallee, R. 1982. A taxol-dependent procedure for the isolation of microtubules and microtubule-associated proteins. *J. Cell Biol.* 92:435–442.
48. Vallee, R., and G. S. Bloom. 1984. High molecular weight microtubule-associated proteins. *Mod. Cell Biol.* 3:21–76.
49. Vandenbunder, B., and G. G. Borisy. 1986. The decoration of microtubules by fluorescently labeled microtubule associated protein 2 (MAP2) does not interfere with interphase organization or progress through mitosis in living fibroblasts. *Cell Mot. Cytoskeleton.* 6:570–579.
50. Vigers, G. P. A., M. Coue, and J. R. McIntosh. 1988. Fluorescent microtubules break up under illumination. *J. Cell Biol.* 107:1011–1024.
51. Wadsworth, P., and E. D. Salmon. 1986. Analysis of the treadmilling model during metaphase of mitosis using fluorescence redistribution after photobleaching. *J. Cell Biol.* 102:1032–1038.
52. Wadsworth, P., and E. D. Salmon. 1986. Microtubule dynamics of mitotic spindles of living cells. *Ann. NY. Acad. Sci.* 466:580–592.
53. Walker, R. A., E. T. O'Brien, N. K. Pryer, M. F. Soboeiro, W. A. Voter, H. P. Erickson, and E. D. Salmon. 1988. Dynamic instability of individual microtubules analyzed by video light microscopy: rate constants and transition frequencies. *J. Cell Biol.* 107:1437–1448.